General Disclaimer

One or more of the Following Statements may affect this Document

- This document has been reproduced from the best copy furnished by the organizational source. It is being released in the interest of making available as much information as possible.

- This document may contain data, which exceeds the sheet parameters. It was furnished in this condition by the organizational source and is the best copy available.

- This document may contain tone-on-tone or color graphs, charts and/or pictures, which have been reproduced in black and white.

- This document is paginated as submitted by the original source.

- Portions of this document are not fully legible due to the historical nature of some of the material. However, it is the best reproduction available from the original submission.

Produced by the NASA Center for Aerospace Information (CASI)

JPL PUBLICATION 78-11

A Probabilistic Model of Insolation for the Mojave Desert Area

(NASA-CR-156140) A PROBABILISTIC MODEL OF INSOLATION FOR THE MOJAVE DESERT AREA (Jet Propulsion Lab.) 36 p HC A03/MF A01 CSCI 04A

N78-20669

Unclas
G3/46 11866



National Aeronautics and Space Administration

Jet Propulsion Laboratory
California Institute of Technology
Pasadena, California

JPL PUBLICATION 78-11

A Probabilistic Model of Insolation for the Mojave Desert Area

O. V. Hester
M. S. Reid

March 1, 1978

National Aeronautics and
Space Administration

Jet Propulsion Laboratory
California Institute of Technology
Pasadena, California

PREFACE

The work described in this report was performed by the Telecommunications Science and Engineering Division of the Jet Propulsion Laboratory.

ACKNOWLEDGEMENTS

The authors would like to express their appreciation for the considerable assistance, suggestions and guidance which they received from Dr. Howard C. Rumsey.

The authors would also like to thank Harry Myers for help with the data reduction.

PRECEDING PAGE BLANK NOT FILMED

ABSTRACT

This report presents a discussion of mathematical models of insolation characteristics suitable for use in analysis of solar energy systems and shows why such models are essential for solar energy system design. A model of solar radiation for the Mojave Desert area is presented with probabilistic and deterministic components which reflect the occurrence and density of clouds and haze, and mimic their effects on both direct and indirect radiation. The model has the capability of producing any or all of the following outputs:

(1) A "clear sky" theoretical amount of solar radiation.

(2) Solar radiation for a clear sky or a cloudy sky or for a sky partially clear and partially cloudy depending on certain probabilistic parameters.

(3) An array of average solar energy reception rates (solar intensities) in kilowatts per square meter (kW/m^2) for a specified length of time.

Multiple comparisons were made between measured total energy received per day and the corresponding simulated totals. The simulated totals were all within 11% of the measured total. The conclusion is that a useful probabilistic model of solar radiation for the Goldstone, California, area of the Mojave Desert has been constructed.

CONTENTS

I. INTRODUCTION ---------- 1-1

II. WHERE AN INSOLATION MODEL IS USED ---------- 2-1

III. THE ASHRAE MODEL ---------- 3-1

IV. INTERACTION OF SOLAR RADIATION AND COLLECTORS ---------- 4-1

V. THE SOLAR MODEL ---------- 5-1

A. INTRODUCTION ---------- 5-1

B. MODEL DESCRIPTION ---------- 5-1

1. Inputs ---------- 5-1

2. Sunrise and Sunset Times ---------- 5-3

3. Expected Number of Dropouts ---------- 5-3

4. Determination of Sky Condition at Sunrise ------- 5-6

5. Simulated Distribution of Duration Times of Dropout and Clear Sky States ---------- 5-7

6. Computation of an Array of Normalized Amplitudes of Dropouts ---------- 5-10

7. Outputs ---------- 5-12

VI. EVALUATION OF THE MODEL AND CONCLUSIONS ---------- 6-1

REFERENCES ---------- 7-1

Figures

5-1. Simplified Flow Diagram of the Solar Model ---------- 5-2

5-2. Pyrheliometer Output for a Cloudless Day ---------- 5-4

5-3. Pyrheliometer Output for a Day With One Dropout ------- 5-5

5-4. Histogram of the Frequency Distribution of Dropouts Per Day From Measured Data ---------- 5-6

5-5. Flow Diagram of the Generation of a Simulated Distribution of Times of Duration of Dropout and Clear Sky States -- 5-8

5-6. Step Function Illustration of a Dropout and a Clear Sky State ---------- 5-9

5-7. Flow Diagram of the Computation of an Array of Normalized Amplitudes of Dropouts ---------- 5-11

6-1. Frequency Distribution of Dropout Times of Duration From the Measured Data ---------- 6-2

6-2. Frequency Distribution of Dropout Magnitudes From the Measured Data ---------- 6-3

6-3. Bivariate Plot of Dropout Amplitude as a Function of Time of Duration for the Measured Data ---------- 6-3

6-4. Bivariate Plot of Dropout Amplitude as a Function of Time of Duration for the First Simulation Run --------- 6-4

6-5. Bivariate Plot of Dropout Amplitude as a Function of Time of Duration for the Second Simulation Run -------- 6-4

6-6. Bivariate Plot of Dropout Amplitude as a Function of Time of Duration for the Third Simulation Run --------- 6-5

6-7. Bivariate Plot of Dropout Amplitude as a Function of Time of Duration for the Fourth Simulation Run -------- 6-5

Tables

6-1. Time-of-Day Distribution of Dropouts for Actual Data and Four Simulations ---------- 6-1

6-2. Actual and Simulated Total Energies. (Also Presented Are the Percentages These Totals Represent of the Actual ---------- 6-6

6-3. Percentages to Which the Energy Totals, (From Table 6-2) Correspond to the Expected Clear Sky Total Produced From the ASHRAE Model ---------- 6-6

SECTION I

INTRODUCTION

After many years of study and experimentation, and in the face of continuing uncertainty over supply and price of conventional energy sources, serious consideration is now being given to the question of using solar-powered energy systems on a relatively large scale. A necessary precursor to construction of well-designed, efficient, and economically viable solar energy systems is the engineering analysis not only of the systems themselves but also of the solar radiation that will drive them. This report presents a discussion of mathematical models of insolation characteristics suitable for use in analysis of solar energy systems and shows why such models are essential for solar energy system design. The currently most-used insolation model is described, as well as the improvements that might be made in it to suit it better for use in designing solar energy systems. The design and construction of an upgraded model is presented together with its preliminary accuracy testing.

SECTION II

WHERE AN INSOLATION MODEL IS USED

Before construction of any energy system is undertaken, there must be reasonable assurance that it will meet the demand it was planned to satisfy, and that it will do so with a low enough life-cycle cost to make the project economically attractive. System performance models can be used first to judge design alternatives against each other and against criteria for performance and cost and then to alter the design of the most promising systems to improve performance and/or lower costs. The function of an insolation model can be better understood by looking at some of the essential features of a solar energy system model.

Solar-powered systems can cover a range of applications, from space and water heating in a single structure to central station generation of electricity, and can vary widely in complexity. A generalized solarthermal system will be made up of solar collectors, possibly some sort of storage subsystem, and a subsystem to convert thermal energy to the desired form. Depending on the application, each of the subsystems might be quite simple or very complex; for illustrative purposes it will be sufficient to think in terms of the general groups. In a gross sense, the energy output of a solar-powered system is determined over a given time period by the amount of solar radiation collected by the system and the overall system efficiency. The efficiency with which the system operates depends in turn on characteristics of the included subsystems and the parameters on which their individual performances will depend.

Of the solar energy hitting a collector, a fraction, depending on the sun's position relative to the collector surface and the collector's own geometry and optical properties, fails to get to the absorbing surface. A portion of the absorbed energy is lost via heat leaks and reradiation; the amount is determined by collector properties and the temperature at which it operates along with other factors like ambient temperature and perhaps wind speed. The remaining energy is transferred from the collector as sensible heat in a fluid at a temperature depending on fluid characteristics, the temperature of fluid entering the collector, and the collector temperature. The temperature of fluid entering the collector depends on how much heat is removed from it by other subsystems, such as that devoted to energy conversion. The amount of heat required by the conversion subsystem is governed by the load it is to satisfy, by its own internal properties, by the temperature of the heat supplied to it, and by the temperature of the sink to which it rejects heat (if it must). The characteristics of the storage subsystem exert an effect on both collector and conversion components. All of these influences are reflected in a subsystem model that is made up of an interrelated set of mathematical models representing the performance of each component. Because each piece depends strongly on factors that vary significantly with time, the resulting model should reflect the important dynamics. Inaccuracies associated with the various component models will propagate and compound during analysis of the system, of course. This means that each of them must represent the performance of

the associated subsystem with greater accuracy than is required of the whole system model.

Given that a system model can be developed that will allow calculation of system output as a function of insolation and other weather parameters, where are we then? A viable energy system, solar or otherwise, must be capable of supplying the output expected of it over the course of its useful lifetime. Conventional systems can be designed with the appropriate capacity and then provided with the amount of fuel necessary to do their job. Fuel for a solar-powered system, sunlight, is completely outside the control of man. Design of a solar energy system--the relative sizing and performance specifications of components--must be done then on the basis not only of its intended output but also on the basis of the energy input that can be expected during its lifetime. The question arises--how does one supply appropriate values for the prime driving function, solar radiation, to allow an estimate to be made of system performance over the span of 10 to 15 future years? That performance analysis must be accurate enough to permit design of a system that meets output criteria and cost criteria in a situation where compensation for even moderate uncertainty by oversizing components can be prohibitively costly.

Experimental measurements of solar radiation intensity could be used to drive a system model. Such measurements are scarce, limited to a few locations, and more often than not of questionable accuracy (Ref. 1). Only rarely, in fact, have the needed aspects of incident radiation been measured. Empirical data suffer from a more fundamental deficiency, however. Using radiation measurements as input for a well-conceived system analysis may give a good estimate of how the system would have performed during the time the data were taken, but that estimate would only be good for the period in which the measurements were recorded. To arrive at the desired system performance it would be necessary, in addition, to simulate the system's behavior over that whole period, a procedure that could be unnecessarily costly and time-consuming.

What is needed is a representation of insolation characteristics that depicts those aspects of both its long-term and short-term behavior on which system performance depends, expressed in terms of a one year description. That one-year description may never match insolation behavior for a particular measured year, but would be extrapolatable to match closely all important aspects of insolation integrated over a long time. The representation would, in short, be the output of a mathematical model describing solar radiation. Such a model, along with a suitable data base, would allow average or representative future behavior to be predicted, along with estimates of the frequency and magnitude of deviations from that average. As noted above, the accuracy of the outputs from this model must be greater than the accuracy required of the outputs of the composite system model.

SECTION III

THE ASHRAE MODEL

An insolation model currently enjoying wide use is that developed by the American Society of Heating, Refrigeration and Air-Conditioning Engineers (ASHRAE) (Ref. 2). It was not created for the purpose of analyzing performance in solar-powered energy systems. Rather, its intended application was in estimating heat load on buildings for the purpose of specifying heating-cooling systems for installation there. The form of the ASHRAE model was dictated by its purpose--this is the case with all mathematical models. In general, the effect of insolation on cooling system requirements is felt on clear sunny days; they specify the conditions with which a cooling system must cope. Only clear days are modeled by the ASHRAE equations.

Some discussion of what happens to sunlight on its way to Earth's surface will aid in dissecting the ASHRAE model. Energy emitted by a point on the sun arrives at the edge of our atmosphere in parallel rays. Its intensity at that point depends on Earth's distance from the sun, and varies slightly with time of year. As the solar radiation passes through the atmosphere, its direct normal intensity (intensity on the plane perpendicular to the ray bundle's direction) is attenuated. Some of the energy is absorbed by molecules of atmospheric constituents and some is figuratively knocked out of the bundle of parallel rays by molecular and particulate scattering. The degree of attenuation from these effects is a function of the distance the radiation has to traverse in the atmosphere, and the concentration of absorbing and scattering species contained there. The ASHRAE model uses the following equation to mimic these influences under clear day conditions:

$$I_{DN} = NAe^{-B/\sin\beta} \qquad (1)$$

I_{DN} is the direct normal intensity of radiation at Earth's surface. N is a clearness number that varies up or down slightly from a value of 1, depending on geographical location and season, and reflects the inevitable variation in clarity of what is considered to be a clear day. The parameter A is classified as apparent radiation at atmosphere's edge; it has a different value for each month and includes the combined influence of the sun's distance from Earth and some atmospheric attenuation. The value of B, the atmospheric extinction coefficient, also varies monthly, reflecting the concentration of absorbing and scattering species. Sets of values for both A and B were determined by empirical curve fitting. That is, they were the values that, when inserted into Eq. (1), produced values of I_{DN} that best matched data actually measured over a long period at a site with a defined clearness number of 1. Finally, $1/\sin\beta$ (where β is the sun's elevation angle) approximates the distance that the parallel bundle of rays travels in the atmosphere, which varies with time of day and time of year.

A unit area of surface at ground level will receive direct radiation I_D at a rate corresponding to the direct normal intensity modified by the cosine of a, the angle between the direction of incoming rays and

the direction perpendicular to the surface.

$$I_D = I_{DN} \cos a \tag{2}$$

In addition to the energy arriving in a direct line from the sun, the surface in question will receive radiation from two other sources. Some of the scattered rays will, after bouncing about in the atmosphere, reach ground level and the receiving surface, coming from all directions. Light that has been reflected from the surroundings will also be picked up. These two effects are treated in the terms

$$I_{DS} = CI_{DN}F_{SS} \tag{3}$$

and

$$I_{DG} = rI_GF_{SG} \tag{4}$$

where I_{DS} is intensity of diffuse radiation coming from the sky, C is an empirically determined factor showing monthly variation, and F_{SS} is a geometrical factor relating to the amount of sky in a position to radiate to the surface. I_{DG} represents radiation reflected onto the surface from the ground around it; I_G is the total radiation intensity falling on the ground (determined as for any surface); r is ground reflectance, and F_{SG} is another geometrical factor. Analogous terms dealing with reflection from other surfaces might be required if the surroundings warranted. To sum up, the total radiation intensity received by a surface near ground level, according to the ASHRAE model, is expressed as

$$I_T = I_{DN} \cos a + CI_{DN}F_{SS} + rI_GF_{SG} \tag{5}$$

When the quantities included are properly evaluated, this model provides good approximations for total radiation intensity as a function of time during clear, that is, cloudless and hazeless, weather. This is one aspect of several needed for accurate analysis of solar system performance.

SECTION IV

INTERACTION OF SOLAR RADIATION AND COLLECTORS

There are many ways of collecting solar energy. As far as their dependence on the characteristics of insolation is concerned, they may be classified in terms of the degree of concentration they involve. While solar energy is intrinsically of high quality, it arrives at Earth's surface widely distributed and must be reconcentrated to be put to useful work. Flat plate collectors use large areas of absorbing material to intercept the radiation as it falls unaltered on the collecting surface. The resulting energy is removed as heat by a fluid circulating over the surface. A flat plate collector can use all the radiation that hits it, but at high operating temperatures heat losses from the large area of hot surface limit its efficiency. Collector designs that concentrate the radiation before it strikes the absorbing surface seek to reduce these heat losses by cutting down on the surface area of hot material, allowing higher efficiency. In effect, the concentrating collectors focus the light on a small absorbing area, from which heat is removed by a circulating fluid. Concentration ratio is a measure of the area over which radiation is captured relative to the area on which it is focused; the higher the concentration ratio the more precise focusing is required.

Only direct radiation is useful to a concentrating collector. The ASHRAE model allows estimation of direct radiation on clear days, where it comprises a large fraction of the total incident light. Energy systems must also work on days that are not entirely clear. Then the proportion of diffuse radiation is much larger, and concentrating collectors will experience their own degradation of output. In comparing systems, one must decide whether large areas of possibly less expensive nonfocusing collectors, with high heat losses but capable of using all the components of incident light, are more or less effective than perhaps smaller arrays of more expensive focusing collectors that will attain high temperatures more efficiently but can't use all the light. This comparison cannct be made without knowing the availability of both direct and diffuse radiation as a function of time for all kinds of days.

The ASHRAE equations embody a semi-empirical, deterministic model. By dealing exclusively with one kind of day, a type that is practically eventless except for the rise and fall of the sun, they can be successfully applied. A requirement for dealing with all days demands a model with probabilistic components as well as deterministic ones. An ideal model will reflect the occurrence and density of clouds and haze, and will mimic their effects on both direct and indirect radiation. For general application to all collectors, another phenomenon must be considered. That is the circumsolar radiation. This is caused mainly by scattering of the sun's rays by Earth's atmosphere, and possibly also by refraction to a smaller extent, and is always present. On clear days, the effect is small and is limited to a narrow angular diameter about the sun's disk. On hazy days the turbidity of the atmosphere increases the circumsolar radiation at the expense of the direct component. It

also increases the angular extent of circumsolar radiation, which then merges with the diffuse radiation. The result is that concentrating collectors cannot focus the sun's disk sharply. Loss from atmospheric defocusing of the sun's image becomes more severe as concentration ratio increases. Neither this effect nor the frequency and nature of unclearness can be modeled deterministically at this time. Random variables must be employed to estimate their influence.

Since the ASHRAE model performs well in predicting radiation on clear days, it forms a sensible starting point for first attempts at constructing a generalized model. We will concentrate on the terms described by Eqs. (1) and (3), regarding the clear-day expressions for direct and diffuse radiation as being a baseline condition that is modified by the random effect of the weather. Modifications would occur via the insertion of a pair of random variables (call them M and m), one in each equation.

$$I_{DN} = MNAe^{-B/\sin\beta} \tag{6}$$

$$I_{DS} = mCI_{DN}F_{SS} \tag{7}$$

Any terms for reflected radiation (Eq. 4) that might be required to model a situation will automatically be modified, since they would be derived from modified estimates of total radiation on the reflecting surface. On a clear day, both M and m would carry values of 1, and the original ASHRAE equations would stand. As "unclearness" increases, the value of M would vary on a short time scale--say, hourly. An additional variable could be inserted into Eq. (6) to model the circumsolar radiation, giving in the end

$$I_D = DMNAe^{-B/\sin\beta} \tag{8}$$

An estimate of how the variable D might depend on concentration ratio has been made, but must be verified. Equations (6) and (8) form a solar radiation model that should be much more suitable than either experimental measurements or the ASHRAE model for supporting engineering analysis of solar energy systems. The improved model will be more representative of solar behavior than a set of measurements, and will deal somehow with all the aspects of radiation that are important to a collector.

The question arises--where do values of M, m, and D come from? Their basis is a series of simultaneous measurements made as accurately as possible in one location over as long a period of time as practicable. The parameters collected would include total insolation intensity and direct radiation as measured by a set of devices with a number of different concentration ratios. Data would be taken at small time intervals, on the order of a few minutes. Diffuse radiation intensity could be derived by differencing measurements of total intensity and direct radiation determined without concentration. These data and Eqs. (6) and (8) would be used to calculate simultaneous values for the three random variables. From the calculated values, a joint probability density function for M and m would be determined, as well as a functional relationship between D and concentration ratio. The derived

probability density functions are used, while model calculations are being carried out, to generate values of the random variables which will lead to a time series of calculated intensities with the same statistical properties as the original measurements.

For probability density functions to give the most representative results, they should be based on a very large number of measurements. It is often the case that their form can be determined from a more limited set of data, after which they can be upgraded by small adjustments in the parameters in which they are expressed as more and more data become available. Modification of the density functions for application to another location may be possible, using a limited number of insolation measurements at the new site and correlation with other weather data that might be more abundant. Verification of such a transfer, and establishment of the conditions under which it would be valid, would require careful measurements for comparison with predicted values.

A program for gathering meteorological and solar data using absolute calibration standards has been underway at the Goldstone Space Communications Complex since June 1974 (Refs. 3, 4, 5). These measurements provide an archive of solar data with calibration traceable to the absolute reference scale established by the Kendall Primary Absolute Cavity Radiometer (PACRAD) II at the World Meteorological Organization Radiometer Intercomparison at Davos, Switzerland, in 1975. Irradiance measurements referred to this scale are found to be numerically 2.1% greater than those same measurements referred to the 1956 International Pyrheliometric Scale (IPS-1956). In addition, the Goldstone measurements provide a data base that has allowed the development of a preliminary solar model such as the one sketched, which is described in the following sections. It must be kept in mind, however, that the approach to an accurate insolation model described in these paragraphs is only a beginning. This probabilistic model is still very much simplified, and future effort might profitably be spent investigating those factors, now determined empirically, to more precisely identify and separate their deterministic and probabilistic components.

SECTION V

THE SOLAR MODEL

A. INTRODUCTION

The mathematical model simulates solar radiation for the Goldstone area and has the capability of producing any or all of the following outputs:

(1) A "clear sky" theoretical amount of direct and total solar radiation.

(2) Direct solar radiation for a clear sky or a cloudy sky or for a sky partially clear and partially cloudy depending on certain probabilistic parameters described below.

(3) An array of average hourly solar energy reception rates (solar intensities) in kilowatts per square meter (kW/m^2) for 1 and 2, above.

The first two can be provided for any desired period of time from 2 minutes to one year. Values are in kilowatt-hours per square meter (kWh/m^2). Averages other than hourly can also be provided by a small modification to the program. If the time period selected is more than a day then daily total insolation values are also provided.

The starting point is the ASHRAE clear day model which has been described above. This clear day model is modulated by the effects of clouds. The distribution of clouds for any given time is determined by the combination of statistical procedures, measured insolation values over a six-month period and a data bank of 19 years of cloud cover information. The method is described in the following sections.

B. MODEL DESCRIPTION

Figure 5-1 is a simplified overall flow-diagram of the model. Each block is explained below.

1. Inputs

The inputs are divided into two kinds; user inputs and built-in inputs. The user must supply information pertaining to the geographical location of interest: station altitude above sea level and station latitude. These data are required in the computation of theoretical clear day insolation levels. The user must also supply the time that he or she is interested in (a single point) or the time interval of interest. The built-in data consist of the theoretical clear day model (ASHRAE model), the measured pyrheliometer data and the weather data. The latter are 19 years of cloud cover and other meteorological data

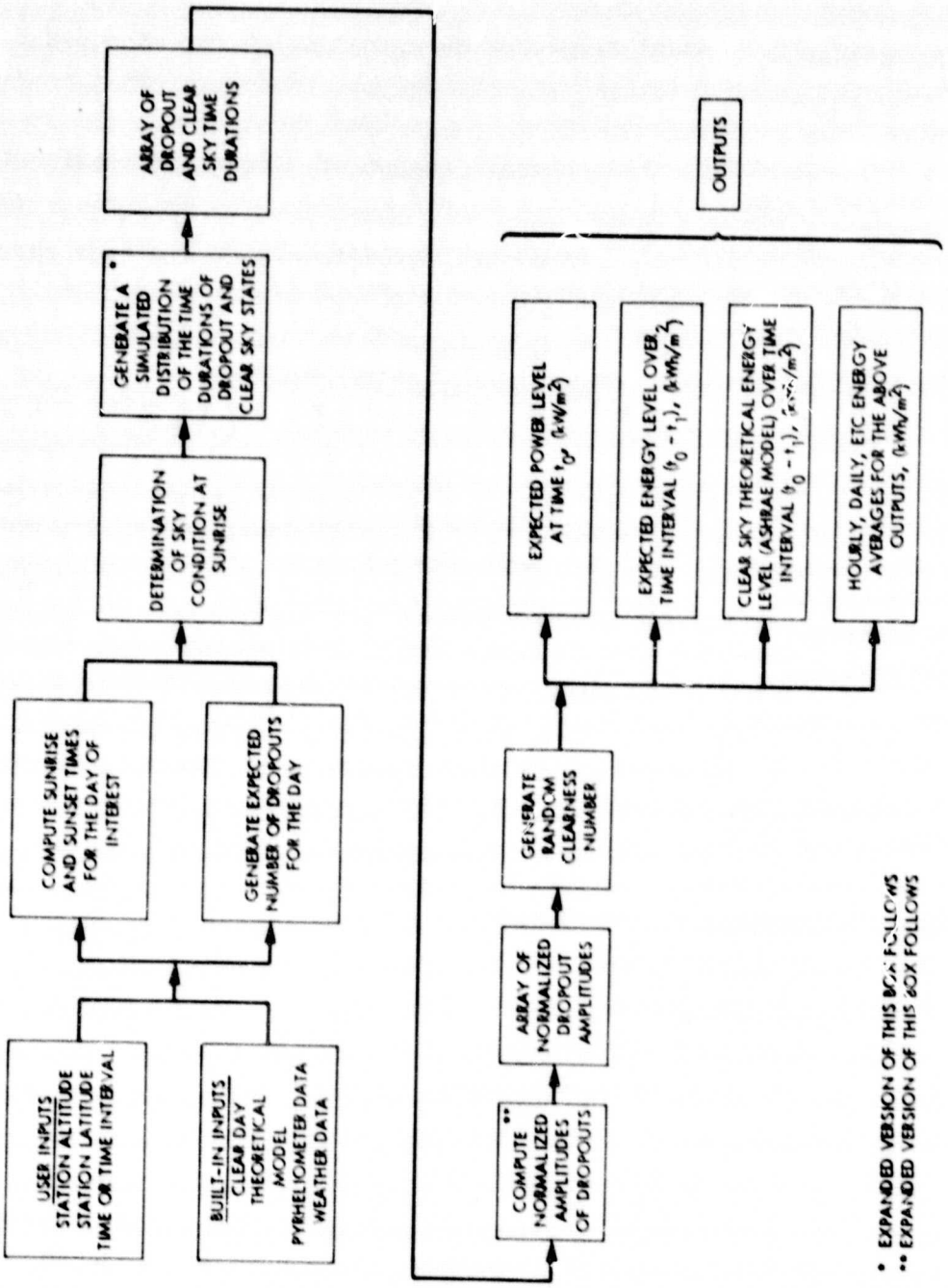


Figure 5-1. Simplified Flow Diagram of the Solar Model

recorded at Edwards Air Force Base, a few tens of kilometers from Goldstone.

2. Sunrise and Sunset Times

Sunrise and sunset times for the day(s) of interest are computed from the ASHRAE model.

3. Expected Number of Dropouts

If a cloud passes between the sun and a pyrheliometer aligned along the direct solar ray the detected insolation level may drop significantly from the clear day level for that instant of time. When the solar intensity drops significantly (5% or more) from the clear day level this is termed a "dropout." Figures 5-2 and 5-3 are plots of the output from a pyrheliometer at Goldstone for two different days in 1975. Figure 5-2 shows a cloudless day and Figure 5-3 shows a day when clouds produced one dropout.

The model computes an expected number of dropouts for the day of interest based on a histogram, made from the measured pyrheliometer data, of the number of dropouts that occurred per day. This number of dropouts is transformed into a continuous variable and is used as an input parameter for computing the expected time durations of dropouts and clear sky states.

It is necessary that the expected number of dropouts be characterized by a continuous function because it is used to generate the expectation parameter of the exponential distribution which is continuous. The discrete distribution of measured dropouts per day from the pyrheliometer data is shown in Figure 5-4. The conversion of this discrete distribution of dropouts per day to a continuous distribution is achieved in the following manner. First, a random selection of an integral number of dropouts per day is made based on the probability distribution of Figure 5-4. Then, with the assumption that the probability of experiencing i to (i+1) dropouts in a single day is uniform, the integral number of dropouts, i, is converted to a random value in the interval i to (i+1). To do this the model simply uses the random number previously generated which determined the interval from i to (i+1) in question. The conversion therefore takes the form:

$$XDOTS = i + \left| \frac{XUNI - P_i}{P_{i+1} - P_i} \right| \qquad (9)$$

where

XDOTS = the expected number of dropouts per day
i = integer part of the expected number of dropouts
XUNI = a random number generated on (0,1)
P_i = the cumulative probability of observing (i+1) dropouts per day

ORIGINAL PAGE IS
OF POOR QUALITY

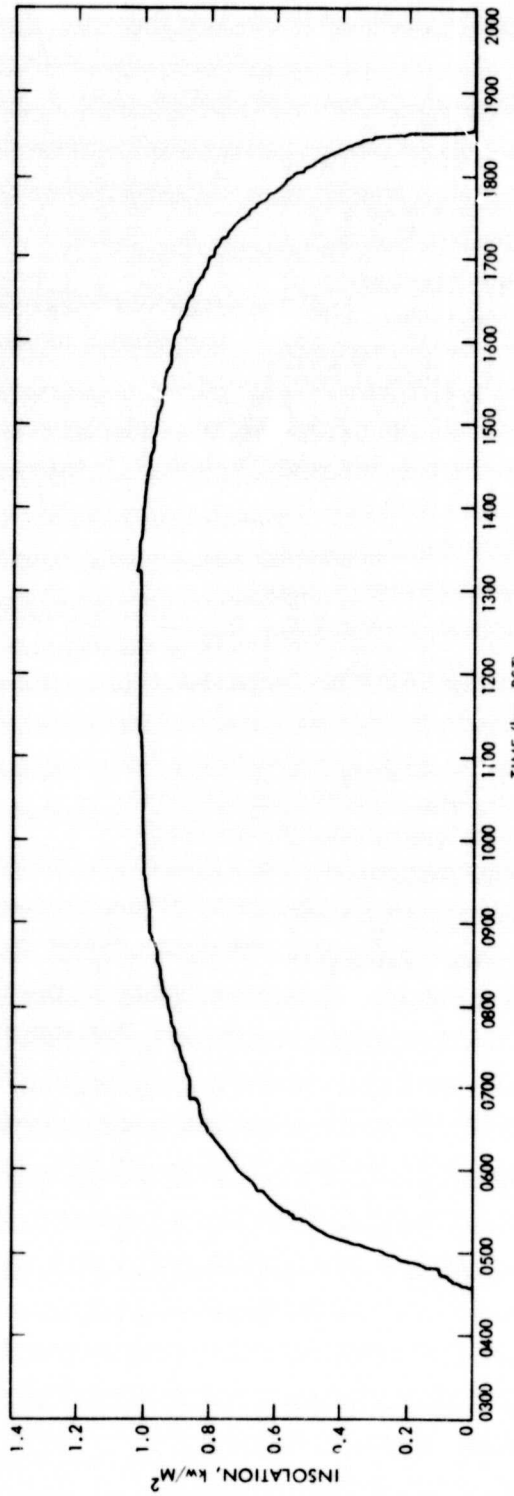


Figure 5-2. Pyrheliometer Output for a Cloudless Day

ORIGINAL PAGE IS
OF POOR QUALITY

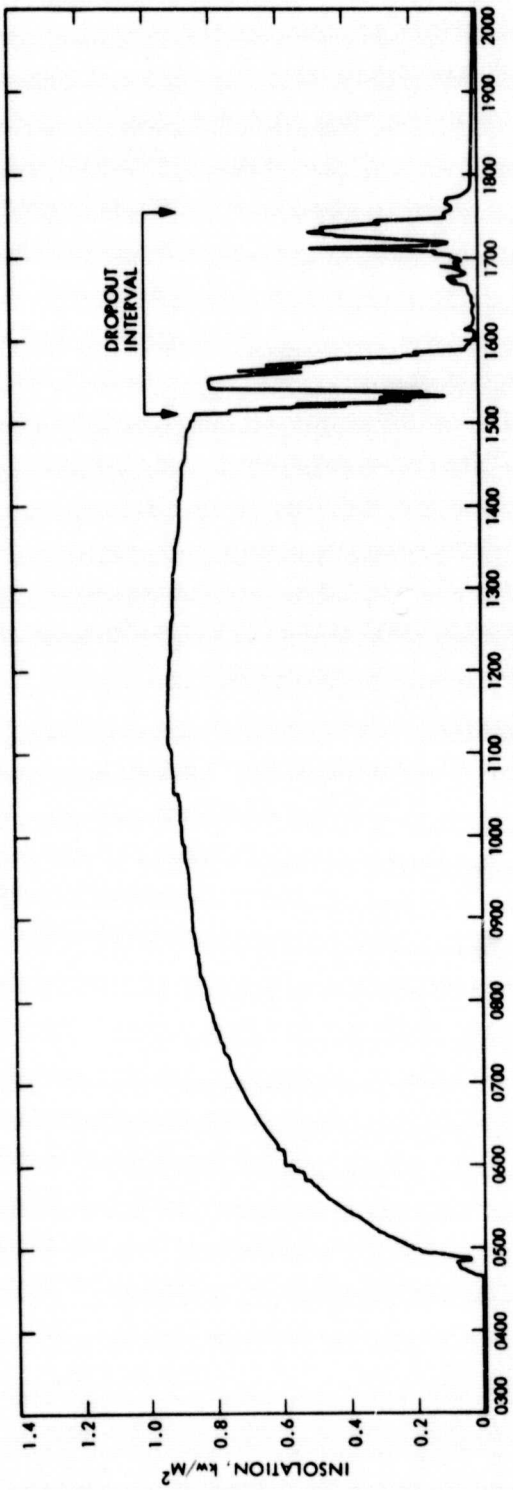


Figure 5-3. Pyrheliometer Output for a Day With One Dropout

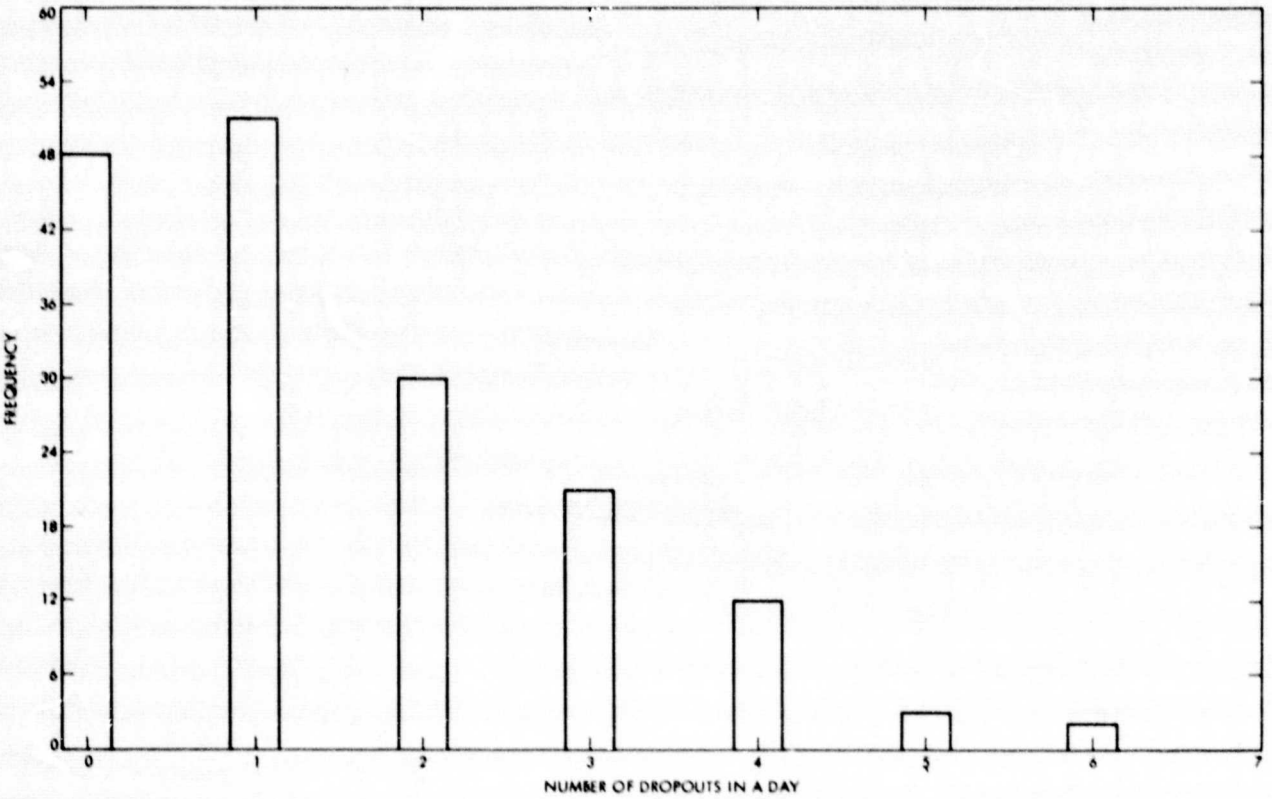


Figure 5-4. Histogram of the Frequency Distribution of Dropouts Per Day From Measured Data

4. Determination of Sky Condition at Sunrise

The solar model steps sequentially through the day of interest from sunrise to sunset and at each step a decision is made whether the direct component of insolation is clear or intercepted by a cloud, and if so how much attenuation is experienced. The time length of the step can be chosen by the user; 5-minute time increments are probably the most convenient and are used in this report. This procedure is used even if the user is interested in only a single point in the day. In order to step sequentially through the day it is necessary to determine the sky condition at sunrise as an initial condition. The weather data input information consists of 19 years of hourly cloud cover data reported as percentages. The percentage cloud cover at sunrise on the day of interest is found from the weather data. The user has the option of choosing a specific year of the weather data, choosing one year of the 19 year set by a random process or using 19 (or other) years averaged data. In any case the hourly data are extrapolated to the exact moment of sunrise. Assume, for example, that decimal percent sky cover at the moment of sunrise on the day of interest is 0.x. The model then generates a random number from the uniform distribution (0,1). If this random number is less than or equal to 0.x then the day of interest starts in a dropout condition. If the random number is greater than 0.x then the day starts in the clear sky condition.

5. Simulated Distribution of Duration Times of Dropout and Clear Sky States

The Flow Diagram of the Solar Model in Figure 5-1 shows that the next procedure is the generation of a simulated distribution of the time durations of dropout and clear sky states. Figure 5-5 is a detailed Flow Diagram of this procedure which is iterated as shown in the figure for each time step throughout the day of interest.

The first step in this procedure is the computation of expected time durations of dropout and clear sky states for a specified time of day, namely the start of each 5 minute time step. Figure 5-6 shows a dropout and a clear sky state symbolically as step functions as they might be recorded from the output from a pyrheliometer. An expected time length of a consecutive pair of dropout and clear sky states is calculated. This time interval is ETOTAL as shown in Figure 5-6 and is given by

$$\text{ETOTAL} = (\text{TDOWN} - \text{TUP})/\text{XDOTS} \tag{10}$$

where TDOWN is sunset time, and TUP is sunrise time and XDOTS is the expected number of dropouts per day computed at the time step of interest. The time interval, ETOTAL, is partitioned into an expected dropout time interval and an expected clear sky time interval, ETIMEDO and ETIMES, respectively. The partitioning is based on the percentage sky cloud cover for the specified time of day from the weather data. Thus:

$$\text{ETIMEDO} = \text{ETOTAL} * \text{PCT} \tag{11}$$

where PCT is the percentage cloud cover (in decimal form) at the specified time. It follows that the time duration of the clear sky state, ETIMES, is given by ETOTAL - ETIMEDO.

At this stage the model has computed expected times of duration of dropout and clear sky states based on the expected number of dropouts (derived from measured data) and the percentage sky cover both of the specified time of day. These expected time lengths, ETIMEDO and ETIMES, are recomputed at each 5 minute time step throughout the sunrise to sunset time interval.

The next block in the Flow Diagram of Figure 5-5 shows that a decision is made whether to continue in the given state or whether to switch states. Both dropout and clear sky state distributions are characterized by the exponential density function.

$$f(t) = \alpha e^{-\alpha t} \tag{12}$$

where t is time and $1/\alpha$ represents the expectation value for the function. The parameter $1/\alpha$ takes on the value of ETIMEDO or ETIMES depending on sky condition--dropout or clear sky, respectively. The exponential density function was chosen because of its property of "lack of memory." That is, the probability of a future event is independent of what happened in the past. Thus the probability of a dropout continuing is independent of how long it has been going on, and similarly for

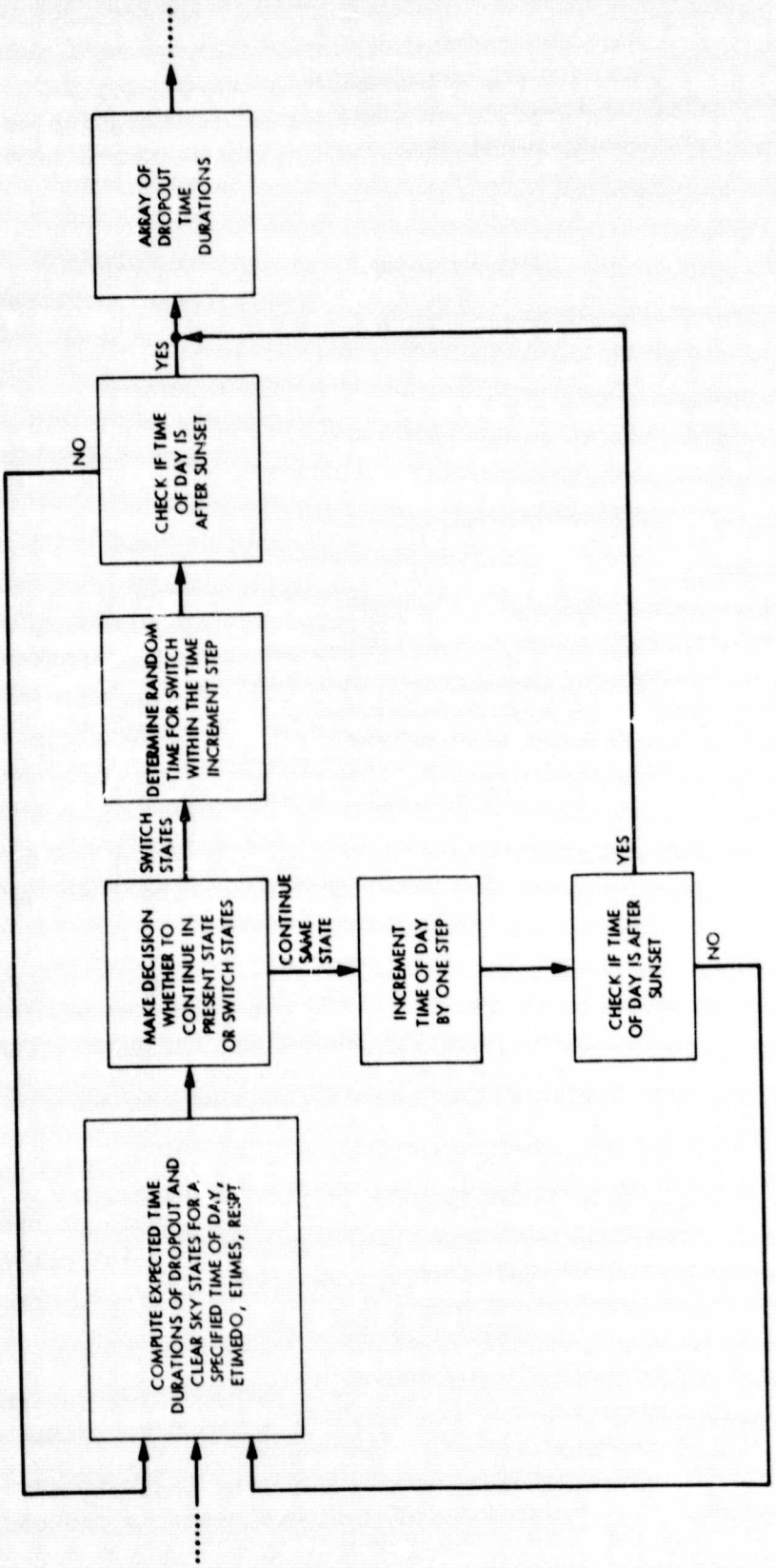


Figure 5-5. Flow Diagram of the Generation of a Simulated Distribution of Times of Duration of Dropout and Clear Sky States

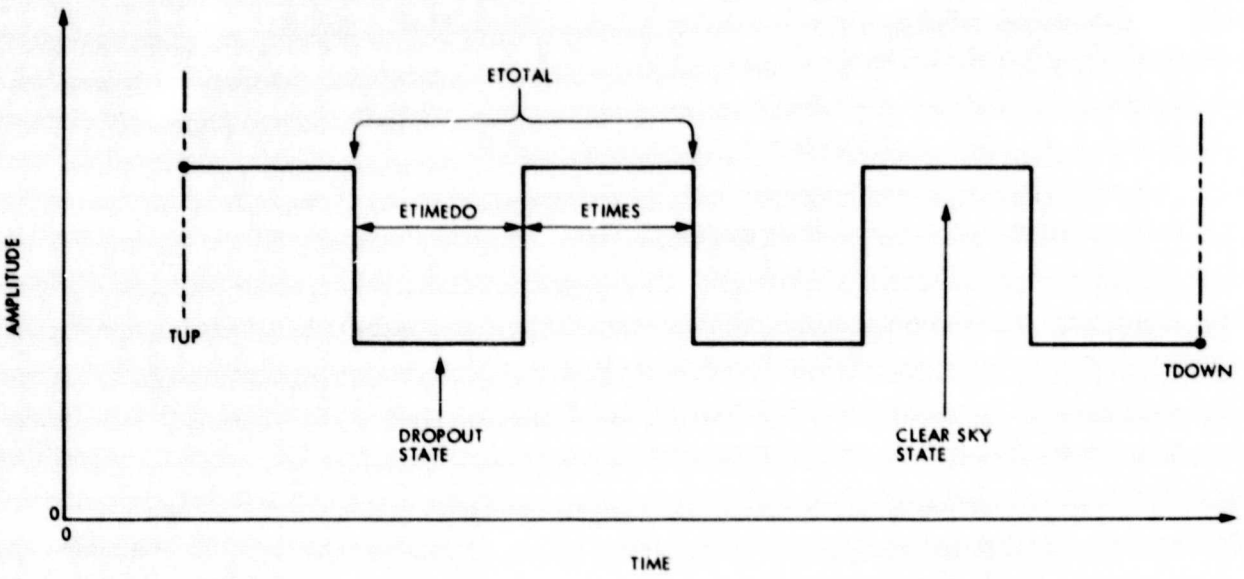


Figure 5-6. Step Function Illustration of a Dropout and a Clear Sky State

a clear sky condition. No findings in the analysis of the measured pyrheliometer data deemed any other distribution more appropriate for the characterization of the two states. Integrating the density function over time (the 5 minute time increment) yields the probability of an event occurring. If, for example, the sky condition is in a dropout state then the integral represents the probability of switching to a clear sky state. Conversely, if the sky were clear it would represent the probability of changing to a dropout condition. These probabilities are obtained directly from the exponential distribution function

$$F(t) = 1 - e^{-\alpha t} \quad t \geq 0 \tag{13}$$

A value for PR, the probability of changing states, is found by substituting into Eq. (13) values for ETIMEDO (if the sky is in a dropout condition) or ETIMES (if the sky is clear) and time, t, (5 minutes). The probability of not changing states is 1 - PR. Next, a random number from the uniform distribution on (0,1), XUNI, is generated. If XUNI is less than or equal to 1 - PR then the sky remains in the given condition, the time of day is advanced by one step of 5 minutes and the procedure is iterated throughout the day.

If XUNI is greater than 1 - PR then the decision is made to switch states. This takes place at some random time in the 5 minute interval. For convenience assume that the sky condition is in a dropout state. The exact instant in the 5 minute interval that the sky changes from a dropout condition to clear is obtained from the inverse function of the exponential distribution function, which is given by

$$t = - [\log(XUNI)] \quad (1/\alpha) \tag{14}$$

where $1/\alpha$ is the present value for ETIMEDO and t presents elapsed time in the 5 minute interval prior to switching states. In Eq. (14) t will always be given by $0 < t < 5$ because a decision to change states corresponds to a value of XUNI given by $1 - PR < XUNI < 1$. Therefore generating a value for XUNI which leads to a decision to change states results in the production of a random time within the 5 minute interval at which the switch is made. The value of t (in minutes) is subsequently added to the time of day corresponding to the beginning of the 5 minute interval and the resulting time represents the end time of the dropout state and the beginning of the clear sky state. This procedure starting with the computation of a percent sky cover, PCT, and an expected time duration of the present state is repeated over the entire sunrise to sunset time, as shown in Figure 5-5. There are certain conditions which, if they exist, cause a deviation from this probabilistic method of deciding when the dropout and clear sky states begin and end. The conditions are:

(1) If the expected time length of whichever state we are in is greater than 0 and less than or equal to 0.001 then the exponent in the distribution function is sufficiently small that the function's value is undefined. Further, the probability of continuing in the state is essentially zero. Therefore, the state is automatically terminated at a random time within the five minute interval.

(2) If the percent sky cover is 1.00 (100%) then the model automatically switches to or remains in the dropout state.

(3) If the percent sky cover is 0 then the model automatically switches to or remains in the clear sky state.

The last box of Figure 5-5 shows that the product of this procedure is an array of time durations, and times of occurrences, of dropout and clear sky states.

6. Computation of an Array of Normalized Amplitudes of Dropouts

The flow diagram of Figure 5-1 shows that the next step is the computation of an array of normalized amplitudes of the dropouts. The normalized amplitude of a dropout is the ratio of the measured energy, in this case the pyrheliometer data, to the clear sky theoretical energy derived from the ASHRAE model. Thus $0 \leq AMP \leq 1$, where AMP is the normalized amplitude of a dropout, and AMP = 1 for a clear sky.

Figure 5-7 shows a flow diagram of the computation of an array of normalized amplitudes of dropouts. A linear regression equation, Eq. (15), of the amplitudes of dropouts on their lengths (time durations) was computed from the measured pyrheliometer data. This regression equation is

$$AMP = 0.44051 + 0.77653\ (TD - 0.06155) \qquad (15)$$

ORIGINAL PAGE IS
OF POOR QUALITY

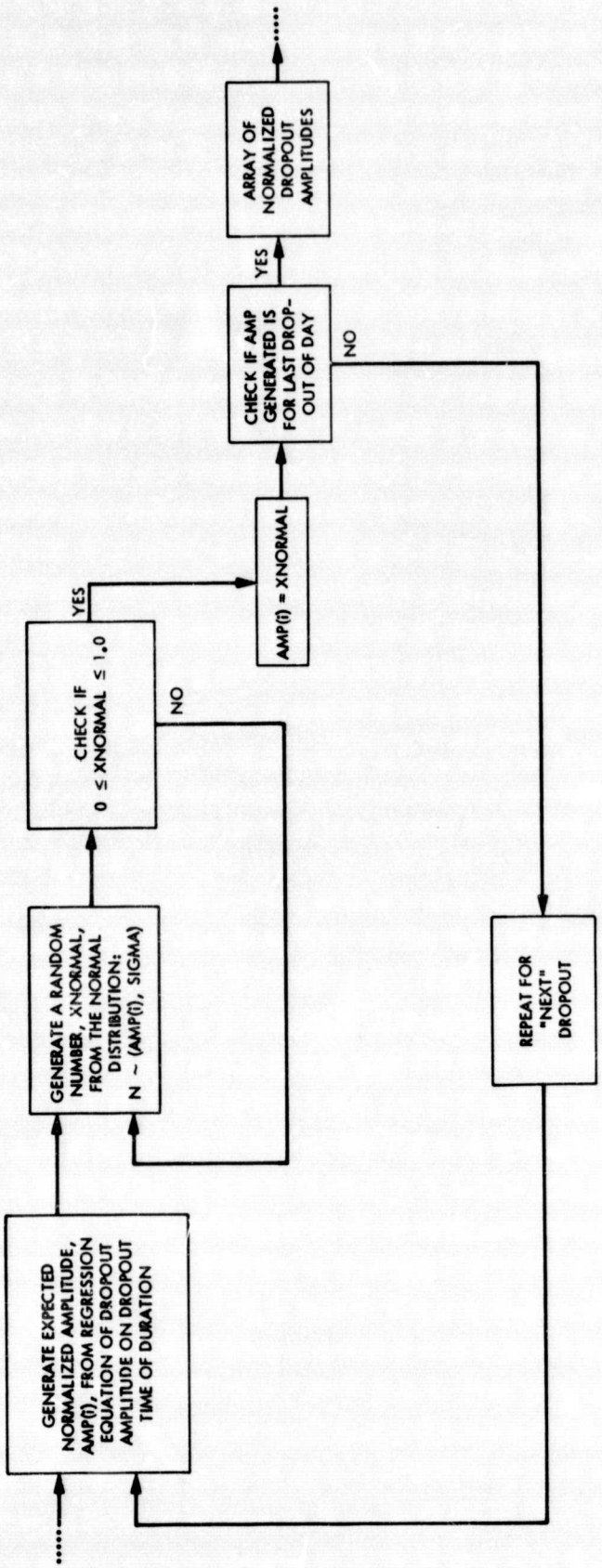


Figure 5-7. Flow Diagram of the Computation of an Array of Normalized Amplitudes of Dropouts

where AMP is the normalized amplitude of the dropouts and TD is their time duration. Expected normalized amplitudes of the dropouts are computed from Eq. (15) using the distribution of dropout time durations found in Figure 5-5.

There was a considerable amount of residual variation at each amplitude level in the measured pyrheliometer data. This residual variation was independent of the time duration of the dropouts and consequently was assumed constant. Furthermore, for a specified time duration the amplitudes of the dropouts were assumed to be normally distributed about the corresponding expected amplitude from the linear regression line. Therefore, after an expected amplitude level for each dropout is obtained from Eq (15) a randomized amplitude level for each dropout is generated from a normal distribution with mean AMP(i) and standard deviation SIGMA. AMP(i) represents the expected amplitude from Eq. (15) and SIGMA is the square root of the residual variation from the regression line.

This process is iterated, as shown in Figure 5-7, to form an array of normalized dropout amplitudes for the entire sunrise to sunset time period or interval.

7. Outputs

At this point the Solar Model has characterized the entire day from sunrise to sunset with a set of dropout and clear sky states, their time durations and times of occurrence, and a corresponding set of normalized amplitudes for the dropouts. This information along with the ASHRAE clear sky model can now be used to compute an array of quantities describing the amount of solar radiation available on any given day.

It is known from experience with solar energy instrumentation and measurements at Goldstone that the clearness number in the ASHRAE clear day model, N in Eq. (1), varies from day to day and possibly even within a day. In order to justify the use of the ASHRAE model, an evaluation of its accuracy with respect to the clearness number was made using the six months of measured pyrheliometer data from Goldstone. A random sample of thirty-five clear sky days (no dropouts) was taken from the measured data, and each of these day's data was integrated over the entire day to yield a measured amount of energy received per day. In addition, for each day, a corresponding theoretical amount of energy was computed from the ASHRAE model using the value of 1.05 for the clearness number. For each pair of theoretical and measured quantities a ratio was formed as well as an average ratio and standard deviation. On the average the measured radiation was 8.9% less than the theoretical radiation. This corresponds to an average measured to theoretically expected ratio of 0.9113312 with a standard deviation of 0.04964. The average value by which the theoretically expected radiation exceeded the measured radiation can be related to the variability of the atmosphere at Goldstone. To compensate for this effect the Solar Model uses a clearness number N', where N' comes from a normal distribution with mean 0.95690 and standard deviation 0.04964, where 0.95690 = (1.05)0.9113312.

A more accurate estimate of the appropriate clearness number of Goldstone represents one area for future improvement of the model.

For each successive time of day a clear sky theoretical solar intensity level (kW/m^2), is computed from the ASHRAE model. This intensity is multiplied by a randomly generated clearness number N' from a normal distribution, as described above. Finally it is multiplied by the normalized amplitude value corresponding to the current time of day. This results in a solar intensity level for the specified time of day. The model treats each intensity level as if it were constant over a one minute time interval. By multiplying each intensity level by one minute the model computes the energy (kWh/m^2) received each minute of the day. Integration over the day, or over any time interval ($t_1 - t_0$) yields the solar energy received in that period. Figure 5-1 shows the various possible outputs.

SECTION VI

EVALUATION OF THE MODEL AND CONCLUSIONS

The frequency distribution of the number of dropouts per day from the measured data was presented in Figure 5-4. Figures 6-1 and 6-2 also present descriptive information on the measured data. Figure 6-1 is a frequency distribution of dropout times of duration computed from the measured data. Figure 6-2 shows the frequency distribution of the dropout magnitudes, also computed from the measured data. A dropout magnitude is defined as

Magnitude = 1 - Normalized Amplitude.

The first step in the evaluation of the Solar Model was to determine if the model produced the appropriate number of dropouts as well as the correct distributions of amplitudes and times of duration. The model was therefore evaluated against the measured data. Figures 6-3 through 6-7 show the actual (from measured data) and four simulated distributions of the dropout amplitudes as a function of their times of duration. It may be seen from the figures that there is a close similarity between the actual and simulated distributions. The total number of dropouts for the actual and the four simulated data sets were: 249, 189, 200, 192, and 187 respectively. The only distinct difference between the actual and simulated distributions was that the actual distribution exhibited a higher frequency of shorter dropouts than the simulated data. This explains the overall number of dropouts being fewer in the simulated data.

A comparison was made between the actual and simulated frequency distributions of dropouts per day, as shown in Table 6-1.

Table 6-1. Time-of-Day Distribution of Dropouts for Actual Data and Four Simulations

	Before 10 a.m.	10 a.m.-2 p.m.	After 2 p.m.
Actual	94	125	143
1st Simulation	91	117	117
2nd Simulation	105	124	113
3rd Simulation	100	104	115
4th Simulation	97	110	118

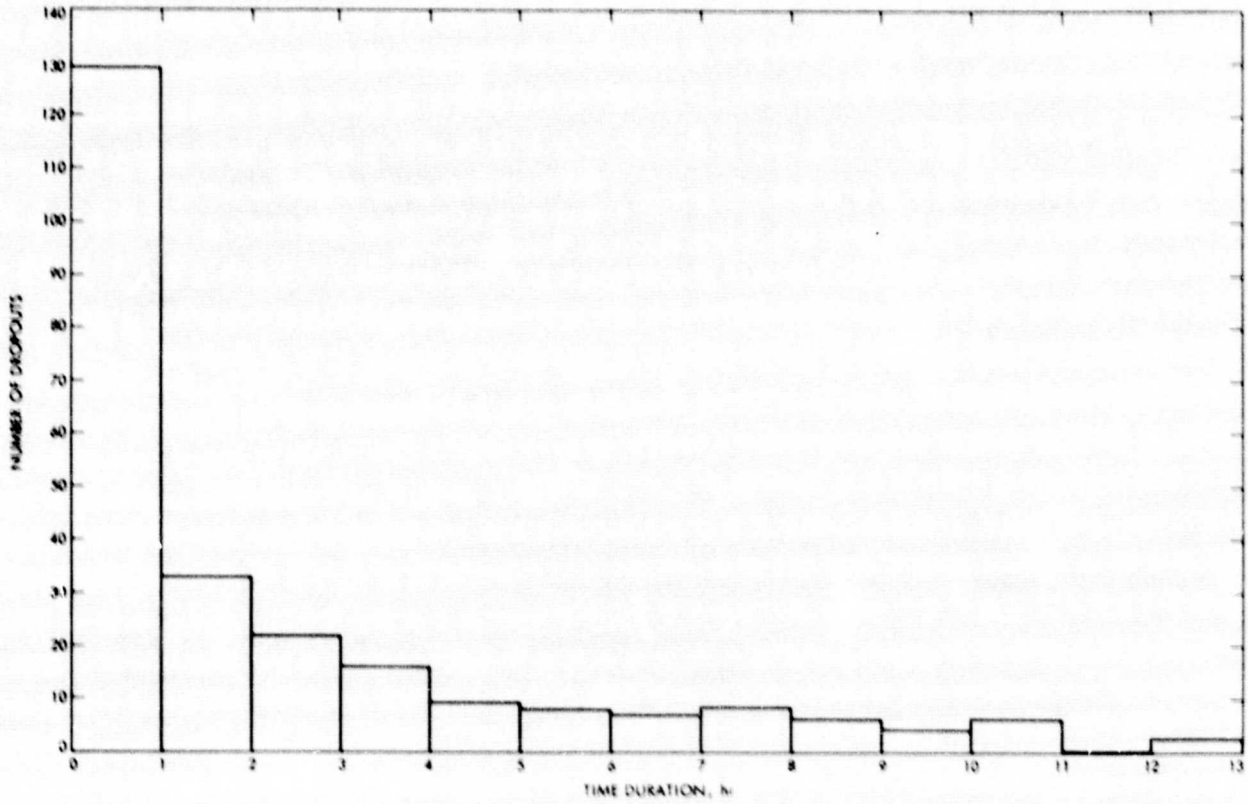


Figure 6-1. Frequency Distribution of Dropout Times of Duration From the Measured Data

If any portion of a dropout was contained in a time interval, the dropout was classified as occurring in that time period. This gives the dropouts the possibility of occurring in more than one time interval and results in a larger expected number of dropouts in the later time intervals of the day. The day was broken up into three time periods: before 10 a.m., between 10 a.m. and 2 p.m., and after 2 p.m. The observed frequency of occurrence of dropouts during these three intervals was 94, 125, and 143 respectively. The uniform increase in the frequency of dropouts occurring in the later times of the day, as expected, coupled with the limited amount of measured data available, led to the decision not to weight the probabilities of dropouts occurring as a function of the time of day. This is another area where future refinement of the model could prove useful.

Multiple comparisons were also made between measured total energy received per day and the corresponding simulated totals. The simulated totals vary because of the probabilistic nature of the model. Table 6-2 is a summary of the actual and simulated data sets. The simulated totals were all within 11% of the measured total. The solar model consistently provided total energies which were conservative estimates of the available energy.

ORIGINAL PAGE IS
OF POOR QUALITY

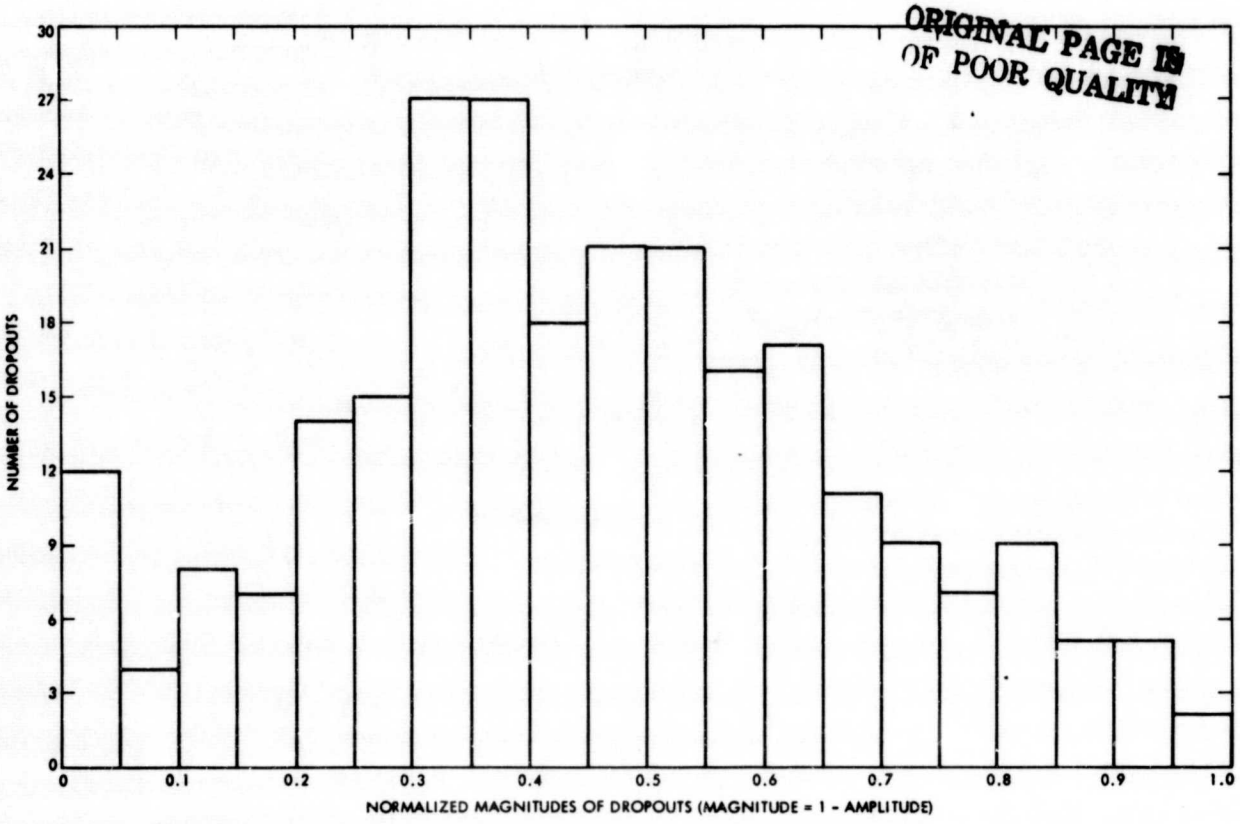


Figure 6-2. Frequency Distribution of Dropout Magnitudes From the Measured Data

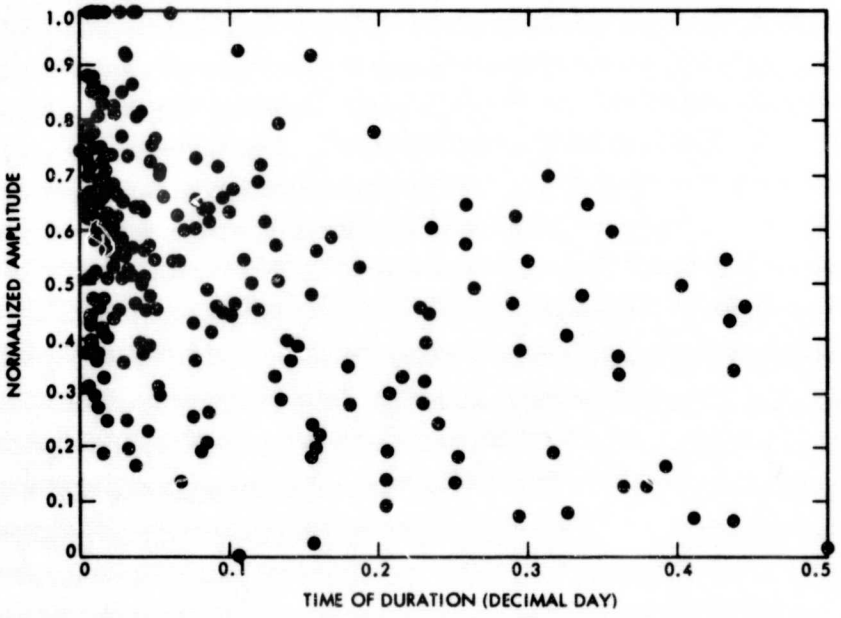


Figure 6-3. Bivariate Plot of Dropout Amplitude as a Function of Time of Duration for the Measured Data

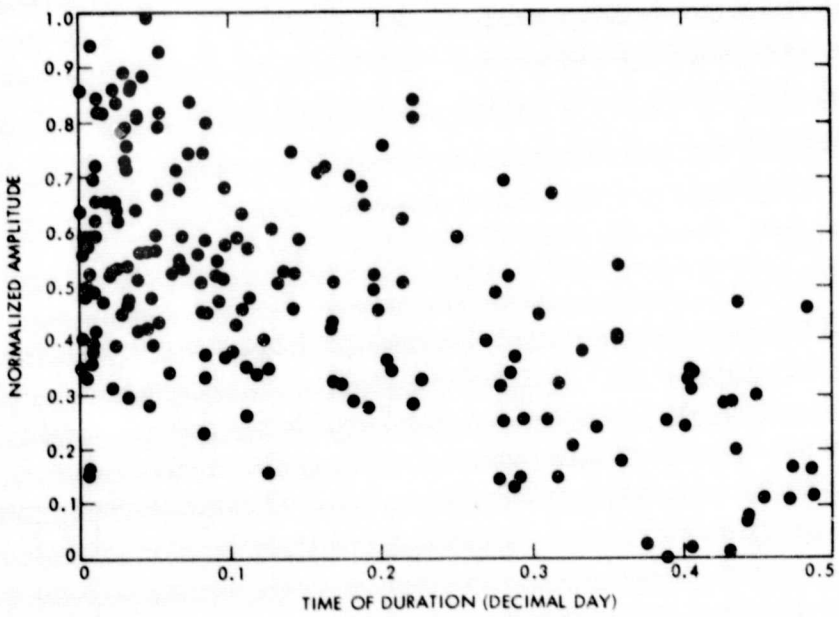


Figure 6-4. Bivariate Plot of Dropout Amplitude as a Function of Time of Duration for the First Simulation Run

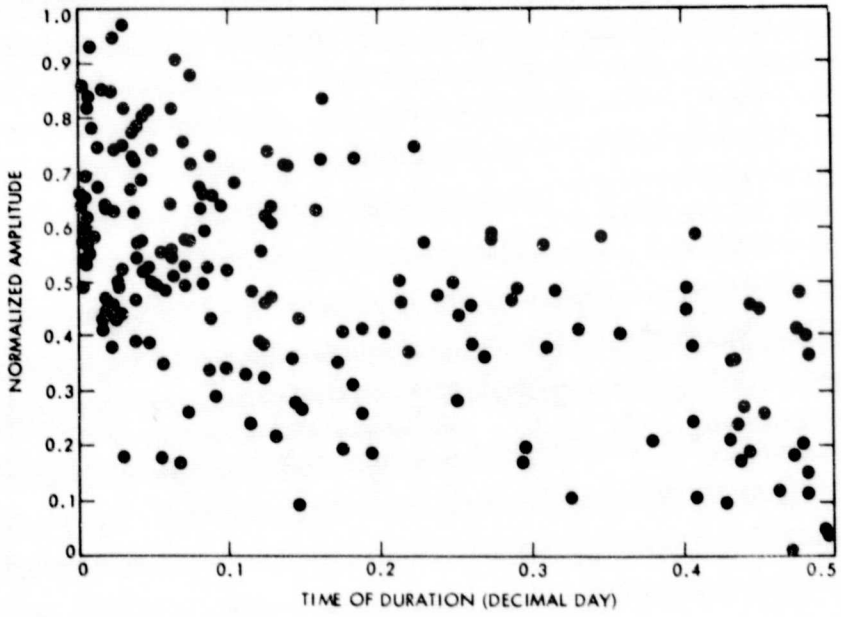


Figure 6-5. Bivariate Plot of Dropout Amplitude as a Function of Time of Duration for the Second Simulation Run

ORIGINAL PAGE IS
OF POOR QUALITY

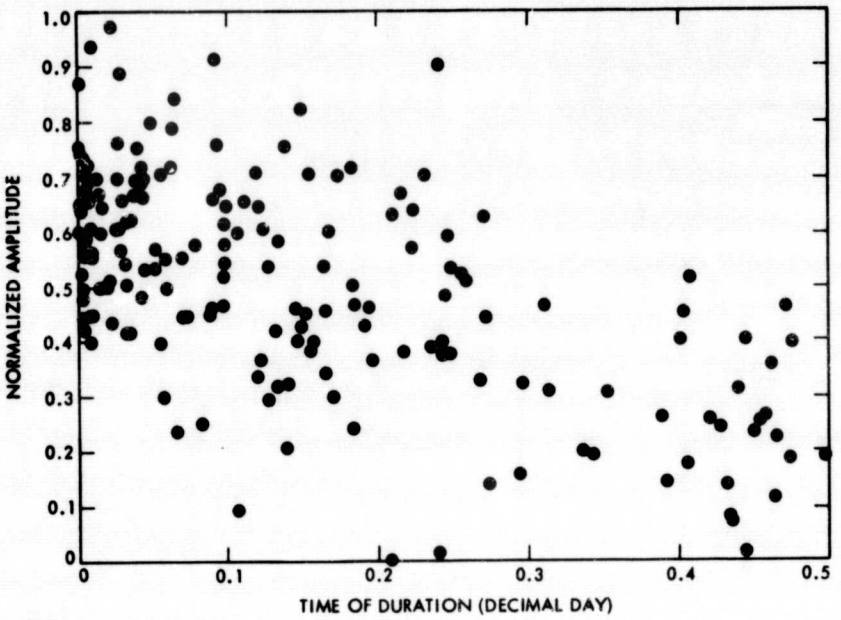


Figure 6-6. Bivariate Plot of Dropout Amplitude as a Function of Time of Duration for the Third Simulation Run

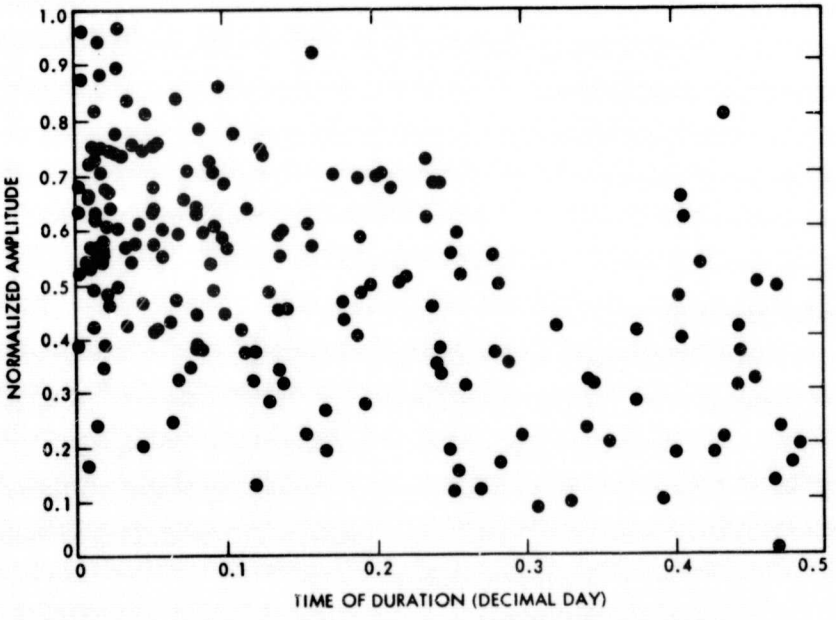


Figure 6-7. Bivariate Plot of Dropout Amplitude as a Function of Time of Duration for the Fourth Simulation Run

Table 6-2. Actual and Simulated Total Energies. (Also Presented Are the Percentages These Totals Represent of the Actual.)

	Total Received Solar Energy kWh/m^2	% of Actual
Actual	733.37	100
1st Simulation	675.53	92.1
2nd Simulation	698.85	95.3
3rd Simulation	661.92	90.3
4th Simulation	658.78	89.8

Table 6-3. Percentages to Which the Energy Totals (From Table 6-2) Correspond to the Expected Clear Sky Total Produced from the ASHRAE Model

	% Clear Sky Total
ASHRAE Clear Sky Total Energy	100.00
Actual	72.1
1st Simulation	66.4
2nd Simulation	68.7
3rd Simulation	65.1
4th Simulation	64.8

Finally, comparisons were made for the sampled days, between the ASHRAE clear sky expected solar energy, and the actual and simulated energy totals. Table 6-3 provides a summary of how these totals compared. The actual energy available observed over the 119 day period represented about 72% of the clear sky expected total, while, consistent with the findings cited in Table 6-2, the simulated energy totals represented slightly smaller percentages. The extreme divergence between the observed and expected clear sky total points to the need for a solar radiation model beyond the capability of the clear sky model for the design, assessment, or analysis of concentrating solar-thermal systems.

Overall the model works well. It must be noted that the model is based on only 6 months of measured data. When more data are available, the model will be improved even thougn it works well and is useful in its present state. The model produces estimates of solar energy which are conservative but this might be improved with further development.

Several areas of refinement for the model were mentioned in the report. These are:

(1) The use of more measured data on which to base the model and characterize the dropouts.

(2) Incorporation of cloud layer data from the weather data in generating dropout amplitudes.

(3) Investigation of the dependence of the probability of dropouts occurring as a function of time of day.

(4) Refinement of the procedure for generating expected time lengths of both dropout and clear sky conditions, which is a critical procedure in the model.

The conclusion is that a useful probabilistic model of solar radiation for the Goldstone area has been constructed. This is a preliminary model which works well and which might be improved in several areas with further work.

REFERENCES

1. Durrenberger, R.W., Brazel, A.J., "Need for a Better Solar Radiation Data Base," Science, Vol. 193, 17 Sept. 1976, pp. 1154-1155.

2. Handbook of Fundamentals. American Society of Heating, Refrigeration and Air-Conditioning Engineers, New York, 1974, Ch. 22, pp 386-394.

3. Reid, M.S., Gardner, R.A., and Parham, O.B., "The Goldstone Solar Energy Instrumentation Project: Description, Instrumentation and Preliminary Results," in The Deep Space Network Progress Report 42-26, pp. 133-144, Jet Propulsion Laboratory, Pasadena, Calif., April 15, 1975.

4. Reid, M.S., and Gardner, R.A., "A Versatile Data Acquisition System for Goldstone," in The Deep Space Network Progress Report 42-30, pp. 132-143, Jet Propulsion Laboratory, Pasadena, Calif., Dec. 15, 1975.

5. Reid, M.S., Berdahl, C.M., Gardner, R.A., "Precision Insolation Measurement Under Field Conditions" Conference Proceedings, Society of Photo-Optical Instrumentation Engineers, San Diego, California, August 1976.